Virchows Archiv A Pathol Anat Histopathol (1988) 412:393–397

Virchows Archiv A
Pathological Anatomy and Histopathology

Case report

Primary rhabdoid tumour of the brain

S.M. Jakate*, H.B. Marsden, and L. Ingram
Department of Pathology and Oncology, Royal Manchester Children's Hospital, Pendleburgy, Manchester, M27 1HA, UK

Summary. A posterior fossa tumour in a 3 year old child is presented with characteristic histological, ultrastructural and immunohistochemical features of rhabdoid tumour. Many tumour cells contained cytoplasmic eosinophilic hyaline inclusions. Ultrastructurally concentric whorls of 10 nm intermediate filaments were identified. Immunohistochemical staining disclosed vimentin, cytokeratin and epithelial membrane antigen positivity. Renal and extrarenal rhabdoid tumours have been well documented but a primary rhabdoid tumour of the brain is extremely rare. Additional ultrastructural features seen were tubular crystalline inclusions in endoplasmic reticulum and abnormal large mitochondria.

Key words: Rhabdoid tumours – Primary brain tumours – Intermediate filaments – Wilms' and related tumours – Vimentin

Introduction

Rhabdoid tumour occurring in the kidney was initially regarded as rhabdomyosarcomatoid variant of Wilms' tumour with poor prognosis (Beckwith and Palmer 1978). It was later identified as a distinctive tumour separate from Wilms' with characteristic ultrastructural features (Haas et al. 1981). The name "rhabdoid" was coined because the tumour cells show eosinophilic cytoplasm simulating rhabdomyoblasts but the ultrastructural and immunohistochemical findings do not support a muscle cell origin.

Primary extrarenal rhabdoid tumours have been described in the liver and chest wall (Gonzalez-Crussi et al. 1982) paravertebral region (Lynch et al. 1983) and soft tissues of the shoulder, neck, arm, perineum and inguinal region (Tsuneyashi et al. 1985). Rhabdoid tumours, renal or extrarenal are highly malignant with consistently poor prognosis.

Recently, Biggs et al. (1987) reported a case of rhabdoid tumour of the central nervous system in a 3 month old boy who died following a two week hospital stay. At autopsy, tumour tissue was present throughout the subarachnoid space of the brain and spinal cord but a predominating intraparenchymal mass in the inferior cerebellum probably represented the site of origin. There have been other reports of cerebral (Briner et al. 1985) and cerebellar (Kapur et al. 1986) rhabdoid tumours. We describe a case of primary rhabdoid occurring in the cerebellum in a child.

Case report

A 3 year old female child presented with unsteadiness of walking and neck pain for 3 weeks associated with early morning vomiting and a squint for 1 week. She had become increasingly lethargic over a month prior to admission. A C.T. scan showed a large mixed density mass lesion in the posterior fossa obliterating the fourth ventricle. The mass showed intense enhancement following contrast and extended anteriorly to involve the leftside of the brain stem. The third and lateral ventricles were markedly enlarged consistent with obstructive hydrocephalus. The full blood counts, serum electrolytes and urine examinations were unremarkable. There was no evidence of a possible renal or extracranial primary tumour.

A posterior fossa exploration was carried out. A tumour occupying the left cerebellar hemisphere was seen to protrude into the fourth ventricle. The tumour was partially removed. Post operatively she had signs of left hemiparesis, VIth and VIIth cranial nerve palsy and palatal paresis of the left side. A C.T. scan showed some resolution of the hydrocephalus but the ventricles were still large. A ventricular-peritoneal shunt was inserted. Following the histopathology report two courses

Offprint requests to: S.M. Jakate, Department of Pathology, University of Leeds, Leeds, LS2 9JT, UK

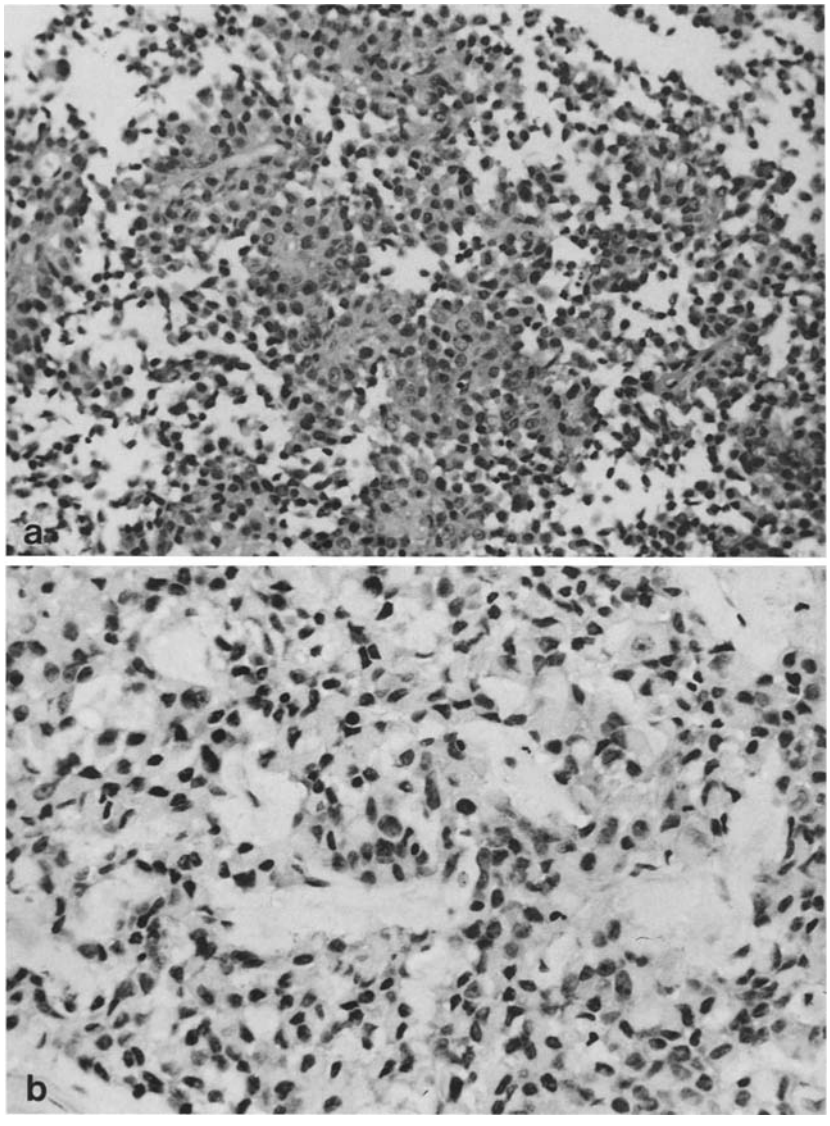

Fig. 1a. Mixture of both diffuse and trabecular patterns in rhabdoid tumour. ×200. **b** Trabecular pattern showing rhabdoid tumour cells with eccentric nuclei and hyaline cytoplasmic inclusions. ×320

of experimental chemotherapy (the 8 in 1 regimen formulated by the International Society of Pædiatric Oncologists) were given along with six weeks of radiotherapy to head and spine. There is marked improvement in neurological function although the follow-up has only been of 5 months.

Material and methods

Multiple tissue fragments were received altogether about 2 cc. For light microscopy fresh tissue was fixed in 10% neutral buffered formalin and processed routinely to paraffin wax. 5 μm cut sections were stained with hæmatoxylin – eosin, Periodic acid Schiff (PAS), PAS with diastase and Gomori reticulin.

Fresh tissue for electron microscopy was fixed in 1% glutaraldehyde in 10% neutral buffered formalin and post-fixed in 1% phosphate buffered osmium tetroxide. Following dehydration and clearing with propylene oxide, tissue blocks were embedded in Emix epoxy resin and cut on an ultramicrotome (LKB ultrotome). Ultrathin sections were stained with uranyl acetate and lead citrate and examined in an electron microscope (Zeiss EM 109).

For immunohistochemistry routinely fixed and processed paraffin sections were taken to phosphate buffered saline (PBS) and endogenous peroxidase was blocked with 3% H_2O_2. Non-specific background was reduced by incubating the sections in normal swine serum (NSS) 1:5 for 20 min. This was tapped off and replaced by anti-glial fibrillary acidic protein (anti-GFAP, Amersham), anti-vementin (Amersham, UK), anti-desmin (Eurodiagnostics BV), anti-cytokeratin – non squamous (Dr. B. Lane, LP 34), anti-neurone specific enolase (anti-NSE, Dako) and anti-epithelial membrane antigen (anti-EMA, Ceralab) in appropriate dilutions and incubated for one and a half hours. The slides were then washed well in PBS and the antibody was detected with swine-anti rabbit (Dako, UK) 1:50 and PAP (Dako, UK) 1:100. The peroxidase was visualised with diaminobenzidine (DAB).

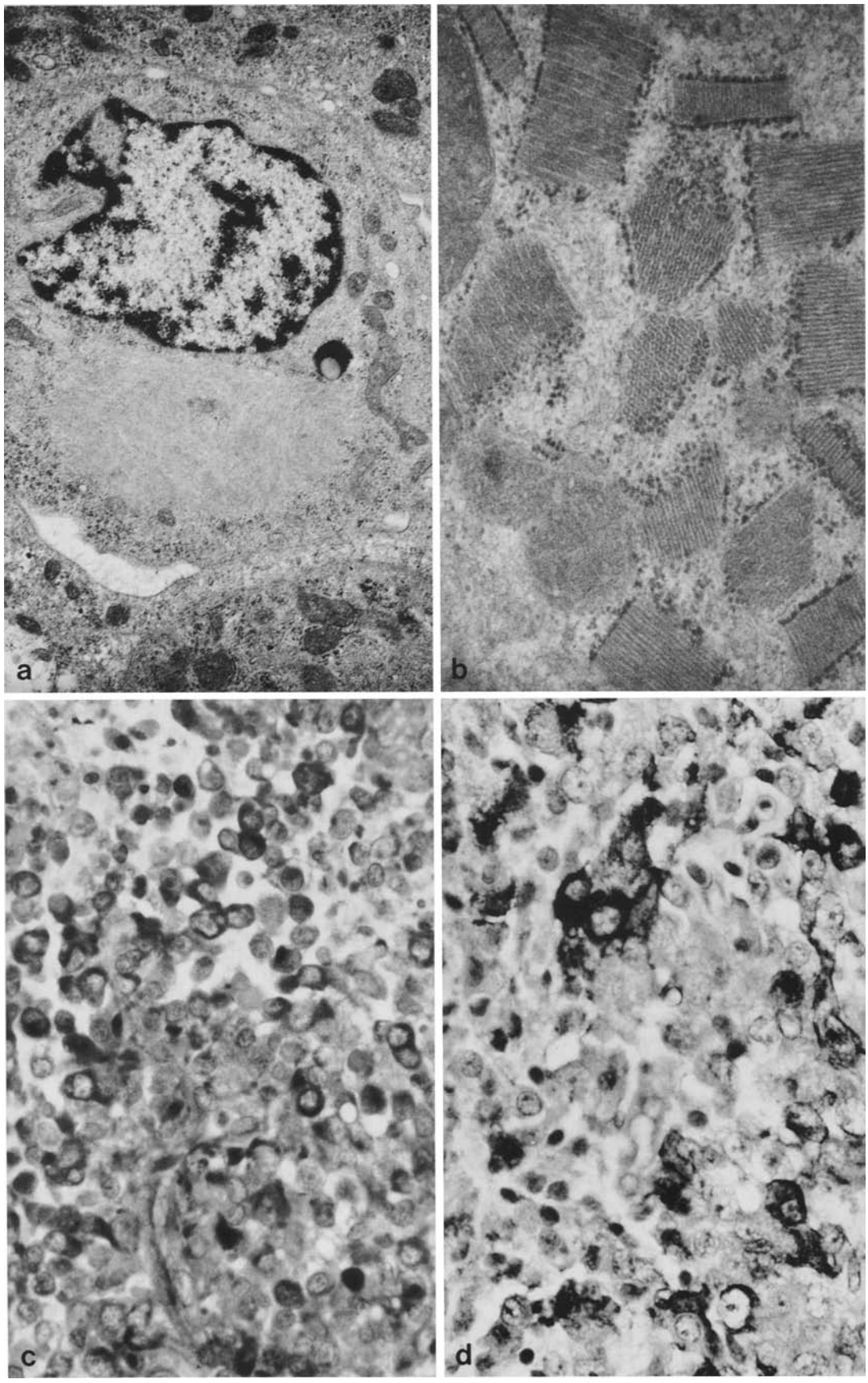

Fig. 2a. Electron micrograph of rhabdoid cell showing eccentric nucleus and paranuclear filamentous mass. ×10240. **b** Crystalline inclusions in the rough endoplasmic reticulum composed of parallel tubules. ×23600. **c** EMA expression by tumour cells. Immunoperoxidase. ×540. **d** Diffuse cytoplasmic vimentin expression by tumour cells. Immunoperoxidase. ×430

Results

Light microscopy

The biopsy fragments consisted entirely of tumour with two main histological patterns. Approximately half the tissue showed diffuse cellular sheets of undifferentiated monomorphic cells. The nuclei were round, vesicular and usually had one prominent central nucleolus. An occasional mitotic figure was seen. The cytoplasm was eosinophilic, generally scanty and the cell margins were indistinct. Isolated thin strands of normal glial tissue intervened between the tumour sheets. A few thick walled vessels were seen with perivascularly arranged tumour cells. Other areas showed nests of loosely arranged cells predominantly in delicate trabecular pattern. Here the nuclei were eccentric, compressed, less vesicular and generally showed a nucleolus. The cytoplasm was abundant, eosinophilic and contained glassy spherical paranuclear masses. The cells margins were distinct (Fig. 1a, b). The stroma was hypocellular and myxomatous. Numerous capillaries traversed the tumour tissue. The two histological patterns merged freely into each other. There was diffuse weak PAS positivity which was diastase sensitive. However, the hyaline paranuclear masses were generally PAS negative. Reticulin fibres were scanty in the compact sheets but moderate in the trabecular areas.

Electron microscopy

The tumour cells were uniformly large and generally oval in shape. The nuclei were mildly irregular and eccentric. Besides the chromatin clumping at the nuclear membranes, the chromatin was scanty and well dispersed. Most of the nucleoli had reticular nucleolonema. The cytoplasm of many cells showed characteristic concentric whorls composed of approximately 10 nm parallel intermediate filaments. These filamentous aggregates were seen in paranuclear area displacing the nucleus and corresponding to the glassy hyaline masses visible on light microscopy (Fig. 2a). There was no evidence of skeletal or smooth muscle differentiation. Scanty to moderate amounts of glycogen, free ribosomes, lipid droplets and rough endoplasmic reticulum were seen. Mitochondria were numerous, some quite irregular and unusually large. Tubular crystalline inclusions were seen in dilated rough endoplasmic reticulum in many cells with 15–20 nm thick parallel tubules (Fig. 2b). No tonofilaments, desmosomes, neurosecretory granules or melanosomes could be demonstrated.

Immunohistochemistry

There was uniform positivity for vimentin (Fig. 2d), nonsquamous cytokeratin and EMA (Fig. 2c). Staining for desmin and NSE was negative. GFAP was demonstrable only in the thin glial strands and not in the tumour cells.

Discussion

Rhabdoid tumours are highly aggressive neoplasms seen in the kidney and extrarenal locations. Extrarenal rhabdoid tumours are seen in infants and adults but in the kidney they occur at a mean age of 13 months (Berry 1987). Renal rhabdoid tumours form about 2% of childhood renal tumours and have a mortality of 90% (Beckwith 1983). Although they were earlier recognised as rhabdomyosarcomatoid variants of Wilms' tumour with unfavourable histology, it is now established that they are distinct neoplasms.

The light microscopic, ultrastructural and immunohistochemical characteristics of rhabdoid tumour have been well documented (Haas et al. 1981; Schmidt et al. 1982; Rutledge et al. 1983; Fung et al. 1981). Light microscopically the tumour shows nests, cords or sheets of cells sometimes with trabecular or perivascular arrangement. Individual cells are generally a mixture of undifferentiated round, polygonal or spindle cells and cells with typical paranuclear glassy eosinophilic inclusions. The nuclei are eccentric, vesicular and many contain one or sometimes more prominent nucleoli. The eosinophilic hyaline inclusions show variable PAS staining reaction, either PAS positive and diastase resistant or PAS negative.

The hallmark of this tumour is the ultrastructural identification of cytoplasmic concentric whorls of intermediate filaments in paranuclear areas in most of the tumour cells. These correspond to the hyaline inclusions seen under light microscope. Occasionally the filaments incorporate central lipid droplets, mitochondria or fragments of ergatoplasm. Such intermediate filaments are nonspecifically seen in various mesenchymal, APUD and epithelial neoplasms. However predominance of these filamentous whorls, relative absence of other ultrastructural differentiating characteristics and typical light microscopic and immunohistochemical features establishes the diagnosis of this rare tumour. Focal dense bodies, scanty tonofilaments and desmosomes have been observed in some cases of rhabdoid tumour but local condensations of filaments or primitive Z-bands have never been demonstrated.

Immunohistochemically the rhabdoid tumour shows consistent vimentin and nonsquamous cytokeratin positivity demonstrable in cytoplasmic globular masses as well as nonglobular areas (Vogel et al. 1984). EMA has been noted to be positive (Kumar et al. 1986). Myoglobin, desmin, NSE, S-100 and alpha-1-antitrypsin are negative.

Our case showing a primary tumour in the cerebellum is admittedly an extremely rare site for a rhabdoid tumour. There is no resemblance to glial or any other known primary brain tumour. It satisfies all the light and electron microscopic and immunohistochemical criteria assigned to rhabdoid tumours. Our case also shows large irregular mitochondria and tubular crystalline inclusions in rough endoplasmic reticulum. These crystalline structures are likely to be proteinaceous secretory products of unknown nature. Among the small numbers of reported cases, primary rhabdoid tumours of the brain appear to originate most frequently from the cerebellum.

Bonnin et al. in 1984 have documented an interesting association of rhabdoid tumours of the kidney with consecutive occurrence of primary tumours in the brain – medulloblastoma, pineoblastoma, cerebral neuroblastoma and malignant subependymal giant cell astrocytoma. Hypercalcæmia has also been seen in association with renal rhabdoid tumours (Rousseau-Merick et al. 1983; Mayers et al. 1984).

The histogenesis of rhabdoid tumour is enigmatic. Neural crest, dual epithelial and mesenchymal and histocytic origins have been suggested. Additional ultrastructural features seen in our case, namely crystalline inclusions in endoplasmic reticulum and abnormal mitochondria, may perhaps contribute towards elucidating histogenesis of this tumour.

Acknowledgements. We are grateful to Dr. S. Kumar for his help in immunohistochemical procedures and Mrs. A. Bolton for secretarial assistance.

References

Beckwith JB (1983) Wilms' tumour and other renal tumours of childhood: A selective review from the National Wilms' Tumour Study Pathology Centre. Human Pathol 14:481–492

Beckwith JB, Palmer NF (1978) Histopathology and prognosis of Wilms' tumour. Cancer 41:1937–1948

Berry PJ (1987) Recent advances in histopathology. No. 13. Churchill, Livingstone, p 216

Biggs PJ, Garen PD, Powers JM, Garvin AJ (1987) Malignant rhabdoid tumour of the central nervous system. Hum Pathol 18:332–337

Bonnin JM, Rubinstein LJ, Palmer NF, Beckwith JB (1984) The association of embryonal tumours originating in the kidney and in the brain. Cancer 54:2137

Briner J, Bannwart F, Kleihues P, Odermatt B, Janzer R, Willi U, Boltshausen E (1985) Malignant small cell tumour of the brain with intermediate filaments – a case of primary cerebral rhabdoid tumours. Pediatr Pathol (abstr) 3:117–118

Fung CHK, Gonzalez-Crussi F, Yonan TN, Martinez N (1981) "Rhabdoid" Wilms' tumour: An ultrastructural study. Arch Pathol Lab Med 105:521–523

Gonzalez-Crussi F, Goldschmidt RA, Hsueh W, Trujillo YP (1982) Infantile sarcoma with intracytoplasmic filamentous inclusions. Distinctive tumour of possible histiocytic origin. Cancer 49:2365–2375

Haas JE, Palmer NF, Weinberg AG, Beckwith JB (1981) Ultrastructure of malignant rhabdoid tumour of the kidney. Hum Pathol 12:646–657

Kapur S, Patterson K, Chandra R (1986) Primary rhabdoid tumour of the cerebellum. Pediatr Pathol (abstr) 5:101

Kumar S, Carr T, Marsden HB, Calabuig-Crepso MC (1986) Study of childhood renal tumours using antisera to fibronectin, laminin and epithelial membrane antigens. J Clin Pathol 39:51–57

Lynch HT, Shurin SB, Dahms BB, Izant RJ, Lynch J, Danes BS (1983) Paravertebral malignant rhabdoid tumour in infancy. In vitro studies of a familial tumour. Cancer 52:290–296

Mayes LC, Kasselberg AG, Roloff JS, Lukens JN (1984) Hypercalcæmia associated with immunoreactive parathyroid hormone in a malignant rhabdoid tumour of the kidney. Cancer 54:882–884

Rousseau-Merck MF, Nogues C, Nezelof C, Marin-Cudraz B, Paulin D (1984) Infantile renal tumours associated with hypercalcanea. Arch Pathol Lab Med 107:311–314

Rutledge J, Beckwith JB, Benjamin D, Haas J (1983) Absence of immunoperoxidase staining for myoglobin in malignant rhabdoid tumour of the kidney. Pediatr Pathol 1:93–98

Schmidt D, Harms D, Ziegler G (1982) Malignant rhabdoid tumour of the kidney. Histology, ultrastructure and comments on differential diagnosis. Virchow Archiv A (Pathol Anat) 398:101–108

Tsuneyoshi M, Daimaru Y, Hashimoto H, Enjoji M (1985) Malignant soft tissue neoplasms with the histological features of renal rhabdoid tumours. An ultrastructural and immunohistochemicl study. Hum Pathol 16:1235–1242

Vogel AM, Gown AM, Caughlan J, Haas JE, Beckwith JB (1984) Rhabdoid tumours of the kidney contain mesenchymal specific and epithelial specific intermediate filaments. Lab Invest 50:232–238

Accepted October 14, 1987